Electronic structure of organobismuth compounds: effective core potential and semiempirical calculations

Lawrence L. Lohr, and Arthur J. Ashe III

More About This Article

The permalink http://dx.doi.org/10.1021/om00026a020 provides access to:

- Links to articles and content related to this article
- Copyright permission to reproduce figures and/or text from this article

Electronic Structure of Organobismuth Compounds: Effective Core Potential and Semiempirical Calculations

Lawrence L. Lohr* and Arthur J. Ashe, III

Department of Chemistry, The University of Michigan, Ann Arbor, Michigan 48109-1055

Electronic structure calculations have been carried out using both effective core potential and relativistically parametrized semiempirical molecular orbital methods for the molecules Bi_2H_4, $C_4H_4Bi^-$, C_4H_4Bi, C_4H_4BiH, and $(C_4H_4Bi)_2$. The latter method has also been used for characterizing one-dimensional chains of $(C_4H_4Bi)_2$ molecules. Key features which are discussed include Bi–C bonding and both intra- and intermolecular Bi–Bi bonding.

Introduction

Suitably substituted distibines and dibismuthines display a dramatic color change (thermochromism) upon melting or dissolution in organic solvents.[1] For example, 2,2′,5,5′-tetramethylbibismole (1) forms deep green crystals
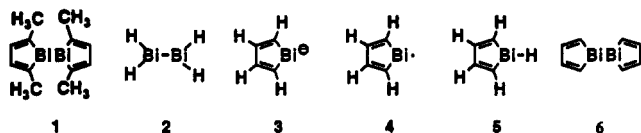
which when dissolved in pentane afford an orange solution.[2,3] Crystal structures of these thermochromic species show the common structural feature that the pnictogen atoms are aligned in chains with short intramolecular bonds alternating with somewhat longer intermolecular contacts.[3–8] The structure of 1 illustrated in Figure 1 is typical.[3] The intermolecular Bi–Bi contact (3.66 Å) is nearly 1 Å shorter than the van der Waals distance (4.6 Å). The close contacts indicate a secondary bonding which is associated with the intense solid-phase color.

Thermochromic distibines, particularly the antimony analog of 1, have been treated by Hoffmann and others using a tight bonding model based on extended Hückel calculations.[9,10] Although dibismuthines have been assumed to be analogous, Buchwald et al. have reported divergent thermochromic behavior for distibines and dibismuthines which bear identical substituents.[11] Since secondary bonding is generally more important for heavier elements,[12] it seems likely that thermochromism should
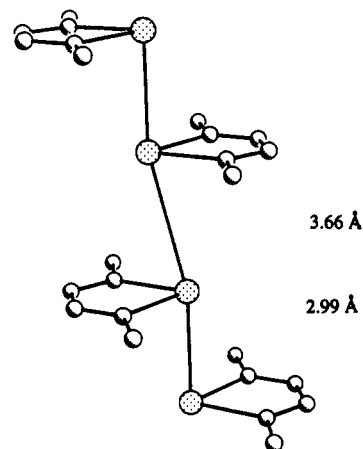
Figure 1. Structure of 2,2′,5,5′-tetramethylbibismole (1), showing the relationship between two molecules along the *a* axis. The unshaded atoms are carbons, while the hydrogen atoms have been omitted for clarity.

be more important for dibismuthines than distibines. Thus, a computational exploration of dibismuthines and analogous organobismuth compounds is desirable.

We report here on electronic structure calculations using both effective core potential and relativistically parametrized semiempirical molecular orbital methods for the molecules Bi_2H_4 (2), $C_4H_4Bi^-$ (3), C_4H_4Bi (4), C_4H_4BiH (5), and $(C_4H_4Bi)_2$ (6).

Methods

Electronic structure calculations were carried out for the molecules Bi_2H_4, $C_4H_4Bi^-$, C_4H_4Bi, C_4H_4BiH, and $(C_4H_4Bi)_2$ using the GAUSSIAN90 program[13] and the effective core potentials (ECP's) associated with the minimal and double-ζ basis sets designated as LANL1MB (MB) and LANL1DZ (DZ), respectively. These ECP's were derived[14] from atomic Hartree–Fock (HF) calculations[15] incorporating the mass–velocity and Darwin relativistic effects but not spin–orbit coupling. For example, unrestricted Hartree–Fock (UHF) calculations using the DZ basis set for the Bi atom yield orbital energies for $6s\alpha$ and $6s\beta$ averaging −18.36 eV, which is close to the numerical Dirac–Fock (DF) value[16] of −18.67 eV but much lower than the completely nonrelativistic

(1) Ashe, A. J., III. *Adv. Organomet. Chem.* **1990**, *30*, 77.

(2) Ashe, A. J., III; Drone, F. J. *Organometallics* **1984**, *3*, 495.

(3) Ashe, A. J., III; Kampf, J. W.; Puranik, D. B.; Al-Taweel, S. M. *Organometallics* **1992**, *11*, 2743.

(4) Ashe, A. J., III; Ludwig, E. G., Jr.; Oleksyszyn, J.; Huffman, J. C. *Organometallics* **1984**, *3*, 337. Mundt, O.; Riffel, H.; Becker, G.; Simon, A. *Z. Naturforsch., B: Anorg. Chem. Org. Chem.* **1984**, *39B*, 317.

(5) Ashe, A. J., III; Butler, W.; Diephouse, T. R. *J. Am. Chem. Soc.* **1981**, *103*, 207.

(6) Becker, G.; Freudenblum, H.; Witthauer, C. *Z. Anorg. Allg. Chem.* **1982**, *492*, 37. Becker, G.; Meiser, M.; Mundt, O.; Weidlein, J. *Ibid.* **1989**, *569*, 62.

(7) Roller, S.; Dräger, M.; Breunig, H. J.; Ates, M.; Gülec, S. *J. Organomet. Chem.* **1987**, *329*, 319; **1989**, *378*, 327.

(8) Mundt, O.; Becker, G.; Rössler, M.; Witthauer, C. *Z. Anorg. Allg. Chem.* **1983**, *506*, 42.

(9) Hughbanks, T.; Hoffmann, R.; Whangbo, M.-H.; Stewart, K. R.; Eisenstein, O.; Canadell, E. *J. Am. Chem. Soc.* **1982**, *104*, 3876.

(10) Ashe, A. J., III; Kausch, C. M.; Eisenstein, O. *Organometallics* **1987**, *6*, 1185.

(11) Spence, R. E. v. H.; Hsu, D. P.; Buchwald, S. L. *Organometallics* **1992**, *11*, 3492.

(12) Alcock, N. W. *Adv. Inorg. Chem. Radiochem.* **1972**, *15*, 1.

(13) Frisch, M. J.; Head-Gordon, M.; Trucks, G. W.; Foresman, J. B.; Schlegel, H. B.; Raghavachari, K.; Robb, M.; Binkley, J. S.; Gonzalez, C.; Defrees, D. J.; Fox, D. J. R.; Whiteside, A.; Seeger, R.; Melius, C. F.; Baker, J.; Martin, R. L.; Kahn, L. R.; Stewart, J. J. P.; Topiol, S.; Pople, J. A. Gaussian, Inc., Pittsburgh, PA, 1990.

(14) Hay, P. J.; Wadt, W. R. *J. Chem. Phys.* **1985**, *82*, 270, 284.

(15) Cowan, R. D.; Griffin, D. C. *J. Opt. Soc. Am.* **1976**, *66*, 1010.

(16) Desclaux, J.-P. *At. Data Nucl. Data Tables* **1973**, *12*, 311.

Table I. Calculated Bond Distances and Angles[a]

molecule	sym	level	Bi–C(2)	Bi–H	Bi–Bi	C(2)–C(3)	C(3)–C(4)	X–Bi–X[b]	C–Bi–X[c]
Bi_2H_4	C_{2h}	HF/LANL1MB		1.753	3.146			91.8	92.0
		HF/LANL1DZ		1.761	2.998			91.2	91.2
$C_4H_4Bi^-$	C_{2v}	HF/LANL1MB	2.208			1.326	1.468	76.9	
		HF/LANL1DZ	2.177			1.372	1.452	78.7	
C_4H_4Bi ($^2B_1$)	C_{2v}	UHF/LANL1DZ	2.191			1.354	1.491	79.2	
C_4H_4BiH	C_s	HF/LANL1MB	2.221	1.756		1.315	1.492	78.2	95.2
		HF/LANL1DZ	2.203	1.762		1.345	1.486	79.0	94.7
$(C_4H_4Bi)_2$	C_{2v}	HF/LANL1MB	2.218		3.186	1.316	1.491	78.3	97.5
		HF/LANL1DZ	2.194		3.058	1.346	1.483	79.2	99.0
	C_{2h}	HF/LANL1MB	2.219		3.181	1.316	1.491	78.2	96.3
		HF/LANL1DZ	2.205		2.986	1.349	1.481	78.6	92.6
		observed[d]	2.23 (1), 2.24 (1)		2.9902 (5)	1.35 (2)	1.44 (2)	79.3 (5)	88.8 (3), 90.0 (3)

[a] All distances in Å and angles in degrees. [b] X denotes H for Bi_2H_4 and C for other molecules [c] X denotes H for C_4H_4BiH and Bi for $(C_4H_4Bi)_2$; for Bi_2H_4, angle is H–Bi–Bi. [d] X-ray distances and angles in the approximately C_{2h} (site symmetry C_i) 2,2',5,5'-tetramethylbibismole.[3]

Table II. Ab Initio Energies, Vibrational Frequencies, Mulliken Charges, and Overlap Populations

molecule	sym	level[a]	energy	imag freq[b]	Bi–Bi freq[c]	Q(Bi)	Q(C(1))[d]	Q(C(2)))	Bi–Bi pop.
Bi_2H_4	C_{2h}	HF/LANL1MB	–12.733 34	14i (a_u)	127	–0.092	0.046		0.418
		HF/LANL1DZ	–12.821 94		124	0.364	–0.182		0.426
$C_4H_4Bi^-$	C_{2v}	HF/LANL1MB	–157.070 50			–0.592	–0.128	–0.017	
		HF/LANL1DZ	–158.982 73			0.143	–0.671	–0.170	
C_4H_4Bi ($^2B_1$)	C_{2v}	UHF/LANL1DZ	–158.974 59			0.742	–0.701	–0.079	
C_4H_4BiH	C_s	HF/LANL1MB	–157.636 99			0.044	–0.130	–0.058	
		HF/LANL1DZ	–159.530 86			0.888	–0.675	–0.089	
$(C_4H_4Bi)_2$	C_{2v}	HF/LANL1MB	–314.201 24	16i (a_2)	117	0.065	–0.126	–0.060	0.390
		HF/LANL1DZ	–317.954 00	35i (a_2)	111	0.695	–0.670	–0.085	0.474
	C_{2h}	HF/LANL1MB	–314.202 17	8i (a_u)	120	0.062	–0.128	–0.057	0.383
		HF/LANL1DZ	–317.963 72		125	0.784	–0.710	–0.096	0.456

[a] Energies in au. [b] Imaginary vibrational frequencies, if any, in cm⁻¹ (symmetry of mode given in parentheses); no entry indicates all real frequencies. [c] Bi–Bi stretching frequency in cm⁻¹. [d] Q(H) for Bi_2H_4.

numerical HF value[16] of –15.19 eV, indicating that the ECP represents well the relativistic stabilization ("inert-pair effect") of the 6s shell. The corresponding DZ orbital energy for 6p is –8.55 eV, not so different from the –7.81 eV weighted mean of the DF values of –9.21 eV for $6p_{1/2}$ and –7.11 eV for $6p_{3/2}$, suggesting that the ECP represents satisfactorily an average over spin–orbit components. Molecular geometries were fully optimized within the constraint of specified molecular symmetries using analytic gradients. Vibrational frequencies were calculated numerically at the resulting stationary points using finite differences of analytic gradients.

To estimate the effects of spin–orbit coupling, calculations were also made using the REX relativistically parameterized semiempirical program[17,18] and the optimized ECP DZ geometries. Both relativistic (REX) and nonrelativistic (EHT) parametrizations were employed for the molecules Bi_2H_4, $C_4H_4Bi^-$, C_4H_4-Bi, C_4H_4BiH, $(C_4H_4Bi)_2$, and $[(C_4H_4Bi)_2]_2$; for the last molecule the ECP DZ geometry for $(C_4H_4Bi)_2$ was used together with an assumed intermolecular Bi–Bi separation of 3.664 Å and assumed collinear Bi atoms (the crystal structure of 2,2',5,5'-tetramethylbibismole indicates a 13.5° tilt of the intramolecular Bi–Bi axis with respect to the intermolecular Bi–Bi axis; Figure 1). These same assumptions were made in our calculations using the related program REXBAND[19,20] for the one-dimensional chain $[(C_4H_4Bi)_2]_x$; REXBAND calculations were also made for a model chain having intra- and intermolecular Bi–Bi separations each equal to 6.650/2 = 3.325 Å.

Results and Discussion

A. As a reference compound for describing Bi–Bi bonds, we considered first dibismuthine Bi_2H_4 (2). The staggered C_{2h} conformation is found (Table I) to have an equilibrium

separation of 2.998 Å with the DZ basis set. Although Bi_2H_4 is unknown, its calculated Bi–Bi separation is virtually identical to the observed separations in solid tetraphenyldibismuthine[21] and 1[3] (2.990 Å). However, the sterically hindered tetrakis(trimethylsilyl)dibismuthine has a somewhat longer separation (3.04 Å).[8] The separation of 3.146 Å calculated for Bi_2H_4 using the MB basis is somewhat too large. The Bi–Bi overlap population (Table II) is approximately 0.42 with either basis, while the Bi–Bi stretching frequency of 124 cm⁻¹ (DZ basis) is almost 15% larger than the value of 110 cm⁻¹ obtained from Raman spectra of several dibismuthines,[22] in line with general computational experience at the SCF level with modest basis sets.

B. In order to explore the Bi–C bonding in $(C_4H_4Bi)_2$ we considered next the monobismuth molecules $C_4H_4Bi^-$ (3), C_4H_4Bi ($^2B_1$ π-radical) (4), and C_4H_4BiH (5). The planar C_{2v} structures of both $C_4H_4Bi^-$ and C_4H_4Bi represent stable equilibria, while C_4H_4BiH is nonplanar, with one H nearly perpendicular to a nearly planar C_4H_4Bi moiety. Selected optimized structural parameters are given in Table I, while energies and selected Mulliken charges are given in Table II.

There are no experimental structural data on 3–5 to compare with the calculated data. However, compounds 1[3] and 7[23] include a 1-substituted bismolyl moiety and thus their observed solid-state structures may be compared with the calculated data for bismole. Similarly bismaferrocene (8)[24] and dibismaferrocene (9)[3] incorporate a

(17) Lohr, L. L.; Pyykkö, P. *Chem. Phys. Lett.* **1979**, *62*, 333.

(18) Lohr, L. L.; Hotokka, M.; Pyykkö, P. *Quantum Chem. Prog. Exch.* **1980**, *12*, 387. The ITEREX-85 program of P. Pyykkö and S. Larsson was also used.

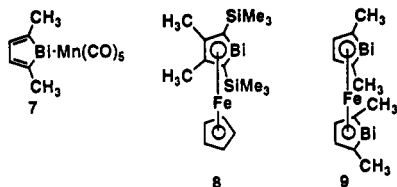(19) Lohr, L. L. *Inorg. Chem.* **1987**, *26*, 2005.

(20) Lohr, L. L. *Int. J. Quantum Chem.: Quantum Chem. Symp.* **1991**, *25*, 121.

(21) Calderazzo, F.; Morvillo, A.; Pelizzi, G.; Poli, R. *J. Chem. Soc., Chem. Commun.* **1983**, 507.

(22) Ashe, A. J., III; Ludwig, E. G., Jr.; Oleksyszyn, J. *Organometallics* **1983**, *2*, 1859.

(23) Ashe, A. J., III; Kampf, J. W.; Puranik, D. B. *J. Organomet. Chem.*, in press.

(24) Ashe, A. J., III; Kampf, J. W.; Al-Taweel, S. M. *J. Am. Chem. Soc.* **1992**, *114*, 372.

metal π-bonded bismolyl moiety. Their solid-state structures may serve as approximate models for **3**.

The DZ structure of bismole is very similar to those of the bismole rings in model compounds **1** and **7**. For **5**, the bond lengths are 2.203 Å for BiC(2), 1.345 Å for C(2)C(3) and 1.486 Å for C(3)C(4), while the average values for the corresponding bonds of **1** and **7** are 2.235, 1.33, and 1.43 Å, respectively. The very acute CBiC angle (78.7°) for **5** nicely matches the 79.3° angle of **7** and the 78.2° angle of **1**. The DZ CBiH angle of 94.3° in C_4H_4BiH falls between the rather divergent average value of CBiBi angle (89.4°) of **1** and the CBiMn angles (98.1°) of **7**. In this respect perhaps, the metal substituted bismoles **7** and **1** are poor models for **5**.

The bismolyl anion $C_4H_4Bi^-$ is of substantial intrinsic interest since it is a heterocyclic analog of the aromatic cyclopentadienyl anion $C_5H_5^-$ (**10**). Qualitatively, π-electron donation from Bi to C is implied by resonance structures (**3b–e**). Relative to the nonaromatic bismole this should have the structural consequence of shortening the BiC(2) and C(3)C(4) bonds while lengthening the C(2)C(3) bond due to changes in the amount of multiple bonding.
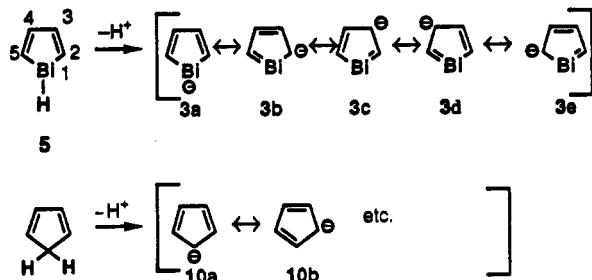
At the DZ level the changes in geometry (Table I) between C_4H_4BiH and $C_4H_4Bi^-$ are ΔBiC(2) = –0.026 Å, ΔC(2)C(3) = +0.027 Å, and ΔC(3)C(4) = –0.034 Å. Thus the data suggest an appreciable aromatic character for the bismolyl anion. Comparison of the bond lengths of the DZ $C_4H_4Bi^-$ with the corresponding bond lengths of the bismaferrocenes **8** and **9** shows only fair agreement (±0.03 Å). Perhaps the transition metal bound bismolyl rings are not good models for the free anion. From the DZ energies in Table II we obtain a HF value of 0.22 eV for the electron affinity (EA) = $-\epsilon(C_4H_4Bi^-$ HOMO) = 0.90 eV, which is probably an upper limit. Similarly, the DZ proton affinity (PA) of $C_4H_4Bi^-$, a measure of the gas-phase acidity of C_4H_4BiH, is 344 kcal mol^{-1}. For comparison we have determined the DZ proton affinity of BiH_2^- as 354 kcal mol^{-1}. The higher acidity of C_4H_4BiH relative to BiH_3 is consistent with an aromatic stabilization of $C_4H_4Bi^-$.

C. The key molecule in our studies is $(C_4H_4Bi)_2$ (**6**), a model for its synthesized 2,2′,5,5′-tetramethyl derivative. The agreement (Table I) between the structural variables calculated with the DZ basis and those observed for the solid tetramethyl derivative is satisfactory with the exception of C(3)C(4) bond distance, which is overesti-
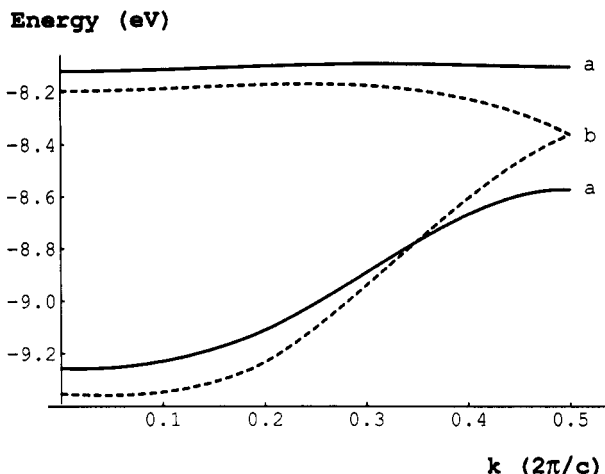

Figure 2. REXBAND HOMO/LUMO energies in eV vs wave vector k in $2\pi/c$ with c = 6.650 Å for $[(C_4H_4Bi)_2]_x$ chains: (a) Bi–Bi = 2.986 Å (intramolecular) and 3.664 Å (intermolecular); (b) Bi–Bi = 3.325 Å (intra- and intermolecular).

mated by 0.05 Å as had been found for **5**. The MB values are comparable except for the computed Bi–Bi separation, which, as with Bi_2H_4, is approximately 0.2 Å too long. The calculated C–Bi–Bi angle is too large by a few degrees but almost identical to the calculated H–Bi–Bi angle for Bi_2H_4. The DZ overlap population of 0.456 for the C_{2h} conformation is slightly larger than the 0.426 Bi_2H_4 value. We find using the DZ basis this C_{2h} conformer to be a local minimum (all real vibrational frequencies), with an energy 6.1 kcal mol^{-1} below that of the eclipsed C_{2v} conformer, the latter having one imaginary frequency corresponding to the torsional mode (a_2) and a rather long Bi–Bi separation of 3.058 Å. With the MB basis, both conformers have an imaginary frequency, although the values are quite small in magnitude (only 8i cm^{-1} for C_{2h}). Recognizing that it is not an accurate measure of the Bi–Bi bond strength, we do note that the DZ ΔHF value for the dissociation energy to form two C_4H_4Bi radicals is 9.1 kcal mol^{-1}. The DZ value of the Bi–Bi stretching mode for the C_{2h} conformer is 125 cm^{-1} (Table II), virtually identical to that calculated for Bi_2H_4.

D. As a complement to our ECP calculations, we have also carried out REX calculations for each of the organobismuth compounds at their optimized HF/LANL1DZ geometries using both the relativistic (REX) and non-relativistic (EHT) parametrizations (Figure 2). Not surprisingly, the noniterative charge distributions (Table III) display greater charge separation than do the ab initio ECP distributions (Table II). The Mulliken charges for Bi are typically 1.0 or greater with either the REX ($6p_{1/2}$ and $6p_{3/2}$ energies of –9.21 and –7.11 eV, respectively) or the EHT (6p energy of –7.79 eV) parametrizations, as Bi is less electronegative than C (2p energy of –11.07 eV). The EHT Bi–Bi overlap populations (Table III) of approximately 0.48 and 0.45 for $(C_4H_4Bi)_2$ with C_{2v} and C_{2h} conformations, respectively, are virtually the same as the DZ ECP values (Table II) of approximately 0.47 and 0.46, respectively, with the REX parametrization values being somewhat less, at approximately 0.39 and 0.38, respectively, suggesting a relativistic weakening of the Bi–Bi bond.

Intermolecular interactions of C_{2h} $(C_4H_4Bi)_2$ units have been modeled in two ways. First, we considered the dimer unit $[(C_4H_4Bi)_2]_2$ with collinear Bi atoms and an assumed intermolecular separation of 3.66 Å, matching that ob-

Table III. Semiempirical Energies, Mulliken Charges, and Overlap Populations

molecule	sym	level[a]	energy[b]	Q(Bi)	Q(C(1))[c]	Q(C(2))	Bi–Bi pop.
Bi_2H_4	C_{2h}	REX	-7.3603	0.66	-0.33		0.551
		EHT	-6.9082	0.70	-0.35		0.622
$C_4H_4Bi^-$	C_{2v}	REX	-15.0744	0.95	-0.83	-0.24	
		EHT	-14.8247	1.03	-0.86	-0.24	
C_4H_4Bi ($^2B_1$)	C_{2v}	REX	-14.7429	1.27	-0.61	-0.12	
		EHT	-14.4848	1.38	-0.67	-0.11	
C_4H_4BiH	C_s	REX	-15.4085	1.30	-0.53	-0.07	
		EHT	-15.1850	1.60	-0.62	-0.11	
$(C_4H_4Bi)_2$	C_{2v}	REX	-29.5360	1.22	-0.59	-0.11	0.358
		EHT	-29.0544	1.45	-0.67	-0.15	0.477
	C_{2h}	REX	-29.5311	1.22	-0.60	-0.11	0.347
		EHT	-29.0408	1.40	-0.66	-0.13	0.447
$[(C_4H_4Bi)_2]_2$[d]	C_{2h}	REX	-59.0622	1.25/1.22[e]	-0.58/-0.62[f]	-0.10/-0.12[f]	0.335/0.061[g]
		EHT	-58.0779	1.45/1.40	-0.66/-0.68	-0.12/-0.14	0.434/0.093

[a] STO basis at HF/LANL1DZ geometries. [b] Energies in au. [c] Q(H) for Bi_2H_4. [d] Assumed distance of 3.66 Å between units along Bi–Bi axis. [e] Bi with and without intermolecular contact, respectively. [f] C's in ring containing Bi with and without intermolecular contact, respectively. [g] Intra- and intermolecular values, respectively.

Table IV. REX HOMO/LUMO Energies[a] for $[(C_4H_4Bi)_2]_n$

$n = 1$	$n = 2$[b]	$n = x$[b,c]	$n = x$[c,d]
-8.13	-8.12	-8.11 ($k = {}^1/_2$)	-8.20 ($k = 0$)
	-8.12	-8.12 ($k = 0$)	-8.36 ($k = {}^1/_2$)
-9.00	-8.81	-8.57 ($k = {}^1/_2$)	-8.36 ($k = {}^1/_2$)
	-9.16	-9.26 ($k = 0$)	-9.35 ($k = 0$)

[a] All energies in eV and based on the HF/LANL1DZ geometry for a $(C_4H_4Bi)_2$ unit with C_{2h} symmetry and Bi–Bi = 2.986 Å except for last column where Bi–Bi = $c/2$ = 3.325 Å. [b] Intermolecular Bi–Bi = 3.664 Å. [c] c = 2.986 + 3.664 = 6.650 Å. [d] Intermolecular and intramolecular Bi–Bi = $c/2$ = 3.325 Å.

served in the solid tetramethylbibismole. The most interesting results are probably the intermolecular Bi–Bi overlap populations (Table III), which are 18 or 21% of the corresponding REX or EHT intramolecular values, thus suggesting modest but not insignificant intermolecular ("secondary") bonding. As another measure of the interaction, we note (Table IV) a 0.35 eV splitting for the dimer of the -9.00 eV HOMO energy of the monomer. Calculations (not tabulated) were also made for the trimer $[(C_4H_4Bi)_2]_3$; the results, including the Bi–Bi overlap populations, are not significantly different from those for the dimer.

For a second model of the intermolecular interactions we considered the one-dimensional chain $[(C_4H_4Bi)_2]_x$, again assuming an intermolecular separation of 3.664 Å, giving a translation distance of c = 2.986 + 3.664 = 6.650 Å. The splitting of the REXBAND HOMO energy as represented by the 0.65 eV difference (Table IV) between the energy at $k = {}^1/_2$ (units of $2\pi/c$) and $k = 0$ is nearly twice the 0.35 eV splitting in the dimer, reflecting the near additivity of the intermolecular interactions. With equalized Bi–Bi separations of 6.640/2 = 3.325 Å, the HOMO–LUMO gap is zero at $k = {}^1/_2$ (Table IV and Figure 1),

corresponding as expected to a one-dimensional metal. We note that the gap of 0.45 eV arising from the band alternation is roughly half of the 0.87 eV gap in the $(C_4H_4Bi)_2$ monomer, or stated differently, the interband gap is comparable to the intraband dispersion.

Summary

Our electronic structure calculations at the ECP level, particularly with the LANL1DZ (DZ) basis set, appear to provide a good description of the geometries of the organobismuth compounds considered. In part this is probably due to the inclusion of the mass–velocity and Darwin relativistic effects in the ECP's, thus providing an adequate representation of the "inert-pair effect". Spin–orbit effects, which are not incorporated in the ECP method, have been estimated using the semiempirical REX and REXBAND procedures, the latter being used to describe linear chains of dibismuthine (6). While appreciable, the atomic spin–orbit splitting of 2.10 eV for Bi (6p) is not sufficiently large as to be dominant over the Bi–C or Bi–H bonding. Secondary Bi–Bi bonding in the dibismuthine chains, as estimated from overlap populations obtained from REX calculation on dibismuthine dimers and trimers, is appreciable, being about 20% of the intramolecular Bi–Bi bonding.